

Mahajneh Allia¹, Piga Isabella¹, Clerici Francesca¹, Capitoli Giulia², Brambilla Virginia³, Galimberti Stefania², Pagni Fabio³, Magni Fulvio¹¹ Clinical Proteomics and Metabolomics Unit, Department of Medicine and Surgery, University of Milano-Bicocca, Veduggio al Lambro, Italy;² Center of Biostatistics for Clinical Epidemiology, Department of Medicine and Surgery, University of Milano-Bicocca, Veduggio al Lambro, Italy;³ Pathology, Department of Medicine and Surgery, University of Milano-Bicocca, San Gerardo Hospital, ASST Monza, Italy

INTRODUCTION

Thyroid nodules diagnosis is performed by fine needle aspiration (FNA) biopsy and approximately only 4–8% are diagnosed as malignant. However, 15–30% of FNABs are indeterminate nodules (THY3), showing insufficient cytological alterations to determine their benignity or malignancy [1]. Today, the debate about the management of these THY3 cases is still open as surgery represents the only possible therapeutic approach. Nevertheless, the post-operative histological evaluation shows that about 80% of THY3 nodules were benign and the surgery could have been avoided [2].

The aim of this work was to apply the MALDI-MSI technique as a new possible diagnostic tool to support the pathologist to improve the triage of thyroid nodules FNAs diagnosis.

METHODS

This work included a cohort of 28 patients, divided in a training and a validation set. The training set was composed of 18 patients: 9 diagnosed as hyperplastic, HP (TIR2), 9 as Papillary Thyroid

Carcinoma, PTC (TIR5). The validation set included the following cytological classes: TIR2 (n=4), TIR3 (n=1), TIR4 (n=1), TIR5 (n=4), plus 1 PTC metastatic lymph node.

All samples were deposited on ITO conductive slides by cyto centrifugation [3]. MALDI matrix (10mg/mL Sinapinic Acid, in 60:40 ACN:H₂O with 0.2% TFA) was uniformly deposited onto the samples using the iMatrixSprayer automated spraying system. All the mass spectra were acquired using a Bruker UltraflexXtreme MALDI-TOF/TOF in linear positive mode within a mass range of 3–20kDa, using a SmartBeam II Nd:YAG/355 nm laser at 2kHz of frequency. After the MALDI MSI analysis, the matrix was removed and the slide were stained with haematoxylin and eosin (H&E). The stained slides were digitally scanned using a ScanScope CS digital scanner and the acquired images were coregistered to the MSI datasets in flexImaging. Regions of interest (ROIs) were selected by the pathologist in order to identify areas with a high density of homogenous cells. Data analysis was performed using the SCiLS Lab software (2019).

CONCLUSIONS

- Regions of interests of thyrocytes can better highlight differences between hyperplastic and PTC
- The classification model correctly classifies the indeterminate lesions (THY3 and THY4)
- The paucity of cells and the presence of inflammatory/colloidal background are confounding factors for the model

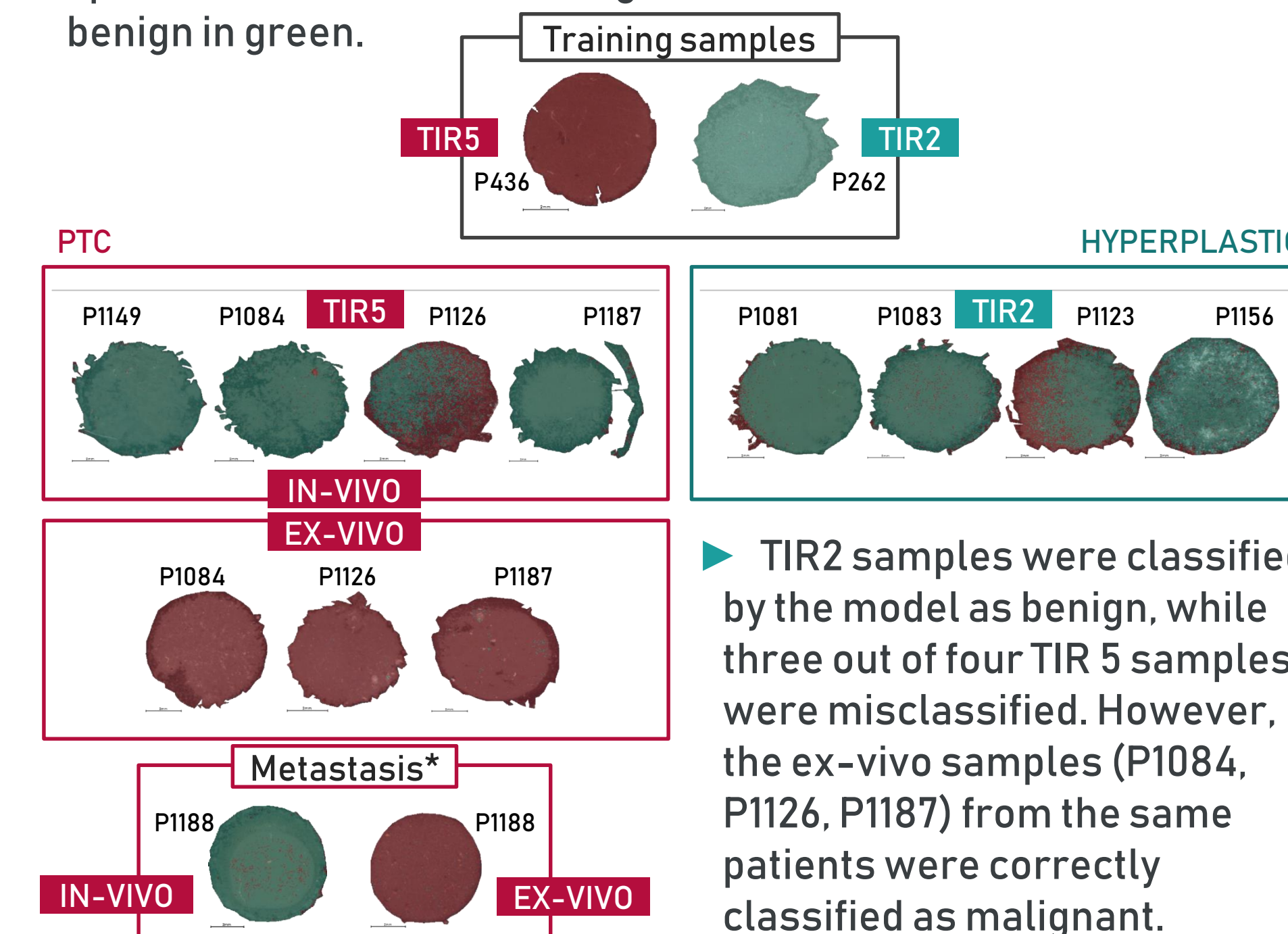
1. F. Nardi, F. Basolo, A. Crescenzi, G. Fadda, A. Frasoldati, F. Orlandi, L. Palombini, E. Papini, M. Zini, A. Pontecorvi, and P. Vitti. *J. Endocrinol. Invest.* 37(6):593–599, Jun 2014.
2. S. Trombetta, G. Attinà, G. Ricci, P. Ialongo, and P. Marini. *International Journal of Surgery* 28:S59–S64, 2016
3. I. Piga, G. Capitoli, S. Tettamanti, V. Denti, A. Smith, C. Chinello, M. Stella, D. Leni, M. Garancini, S. Galimberti, F. Magni, and F. Pagni. *PROTEOMICS – Clinical Applications*, 13(1), 2019.

ACKNOWLEDGEMENTS

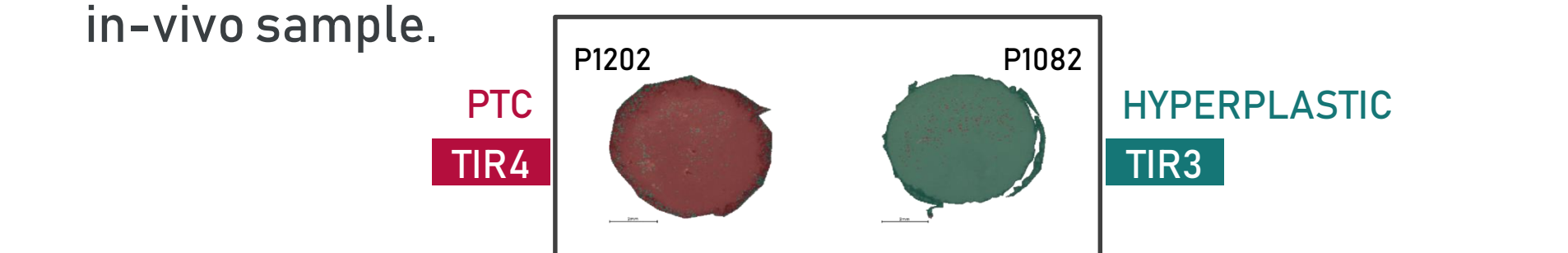
This work received funding from the 2019 Gilead Fellowship Program, AIRC: MFAG GRANT 2016–Id. 18445 and Regione Lombardia POR FESR 2014–2020. Call HUB Ricerca ed Innovazione: ImmunHUB.

RESULTS: Classification

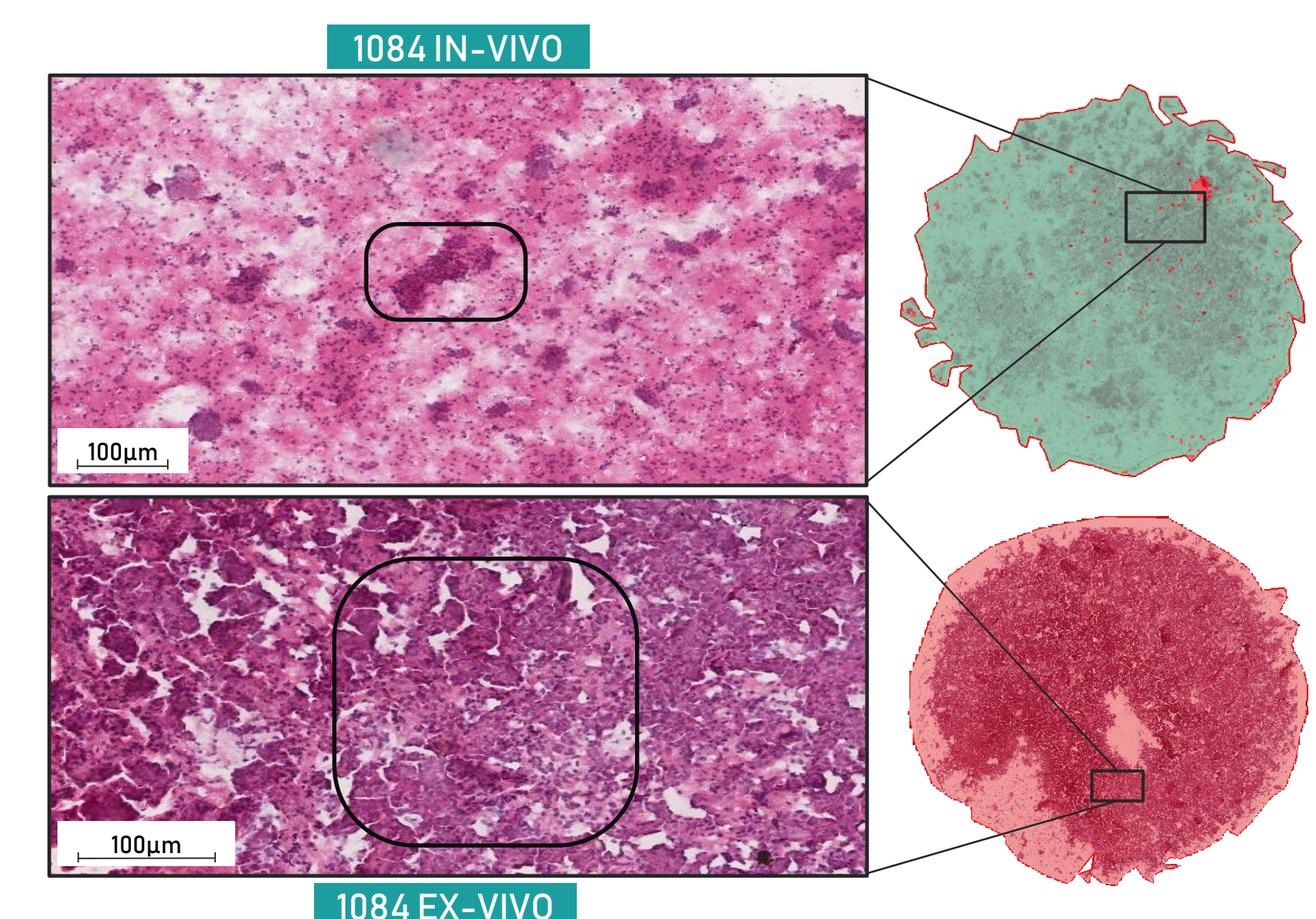
- Pixel by pixel images of training and validation sets. Pixel which spectra are classified as malignant are coloured in red, while benign in green.



- Similarly, the model correctly classified as malignant P1188 ex-vivo from a metastatic lymph node, while still misclassifying the in-vivo sample.

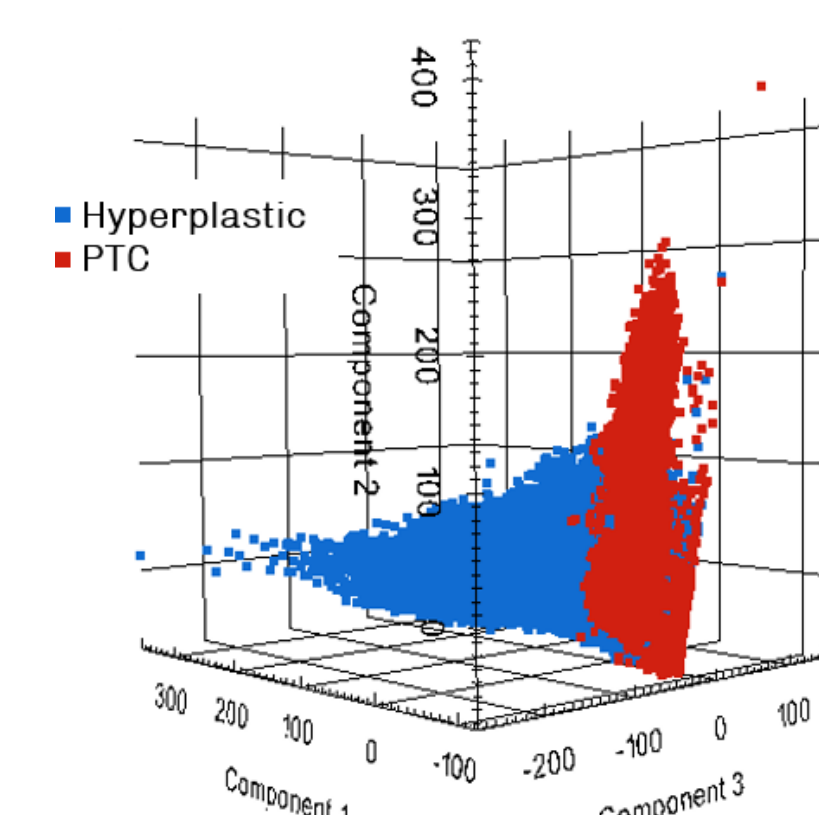


- Lastly, the classification model also correctly classifies the indeterminate lesions (THY3 and THY4).

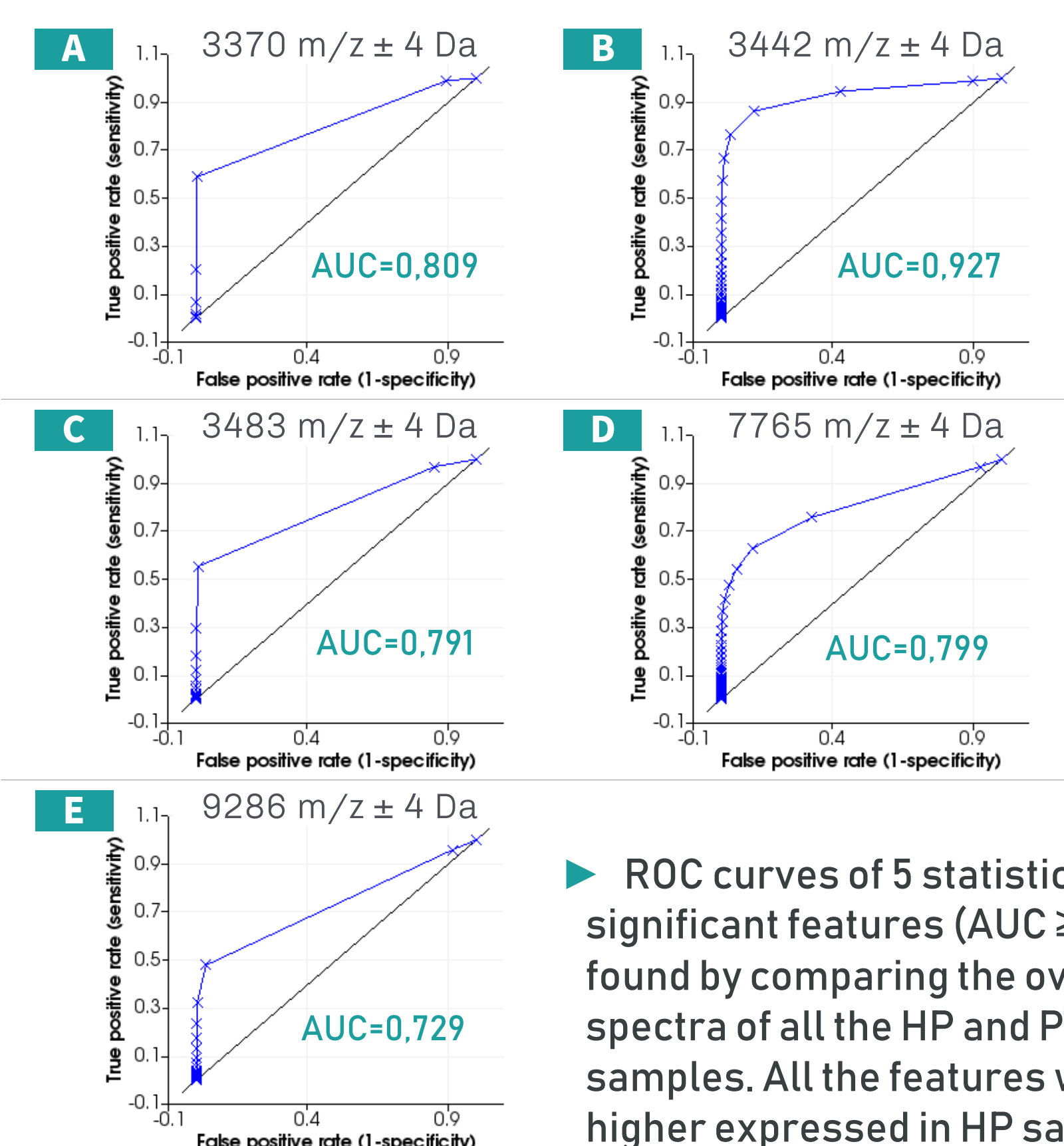


- Haematoxylin and eosin (H&E) staining of 1084 in-vivo and ex-vivo samples. It highlights the different amount of neoplastic clusters (circled in black) between in-vivo and ex-vivo samples.

RESULTS: Overall samples

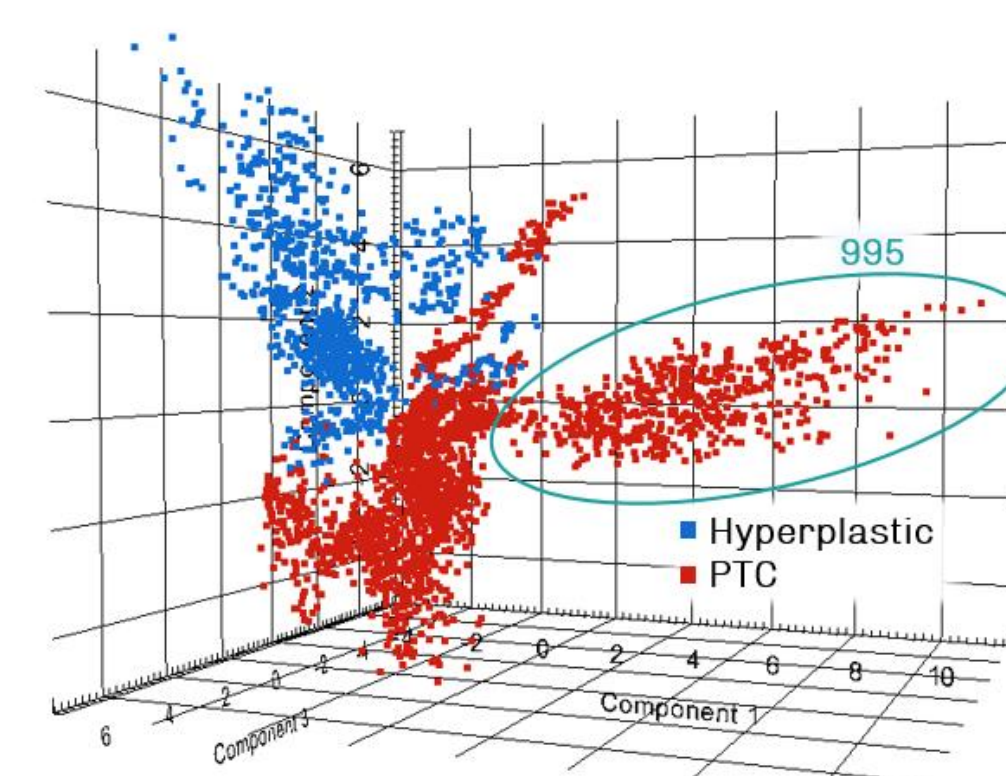


- Protein profile distributions of hyperplastic and PTC samples represented by a 3D PCA score chart, with each pixel representing an individual spectrum. PTC and HP were mostly clustered apart with some grade of overlap due to the common heterogeneous cellular background.

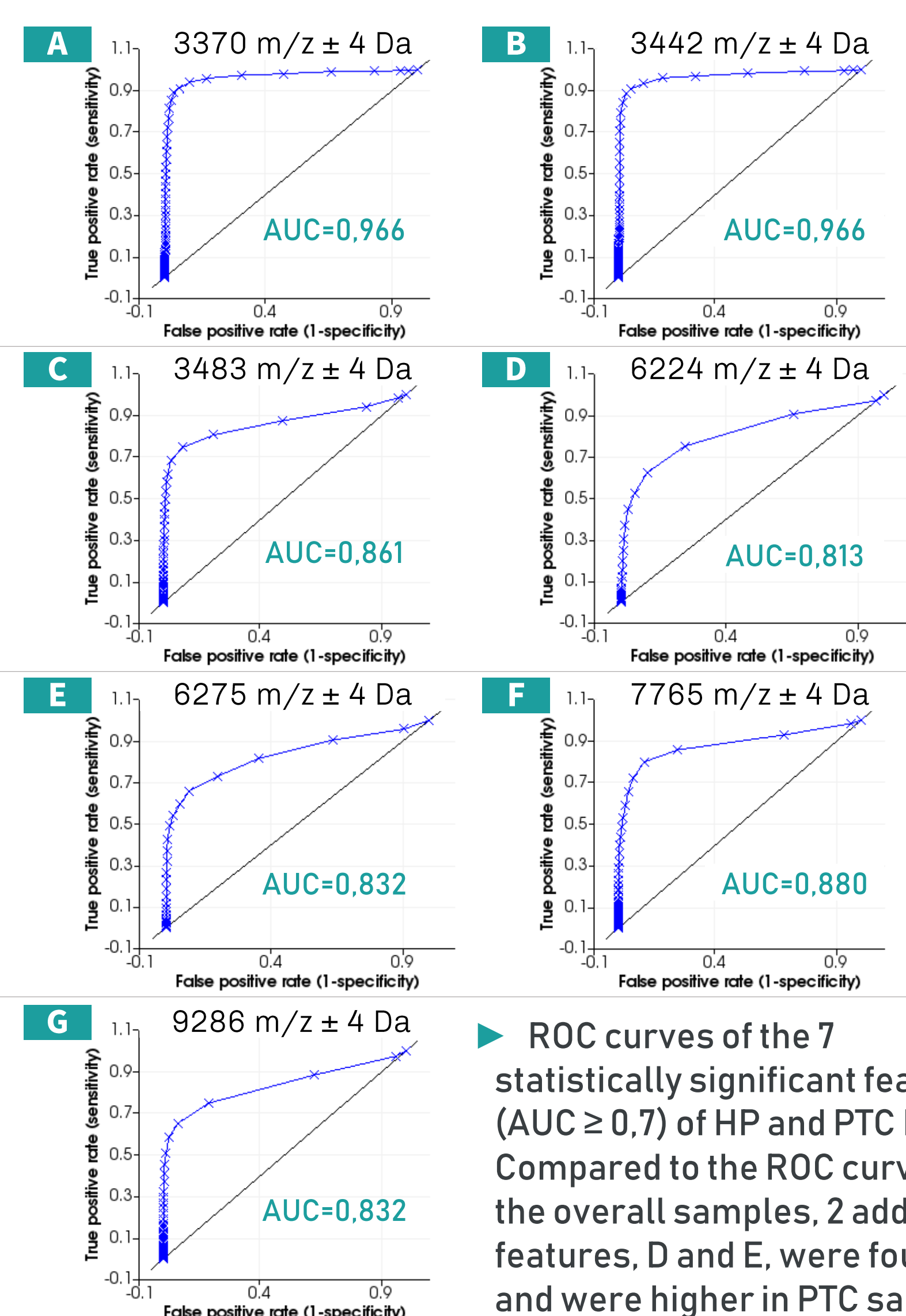


- ROC curves of 5 statistically significant features (AUC ≥ 0.7) found by comparing the overall spectra of all the HP and PTC samples. All the features were higher expressed in HP samples.

RESULTS: Thyrocytes regions



- PCA score chart showing the protein profile distributions of individual spectra from HP and PTC ROIs. Spectra from benign ROIs are clustered together and separated from malignant.



- ROC curves of the 7 statistically significant features (AUC ≥ 0.7) of HP and PTC ROIs. Compared to the ROC curves of the overall samples, 2 additional features, D and E, were found and were higher in PTC samples.

Methods

